Multimodal spectroscopic analysis of the Fe-S clusters of the as-isolated *Escherichia coli* SufBC_2D complex

Giulia Veronesi, Julien Pérard, Martin Clémancey, Catherine Gerez, Yohann Duverger, Isabelle Kieffer, Frédéric Barras, Serge Gambarelli, Geneviève Blondin, Sandrine Ollagnier-De-Choudens

Multimodal spectroscopic analysis of the Fe-S clusters of the as-isolated *Escherichia coli* $SufBC_2D$ complex

Giulia Veronesi[1], Julien Pérard[1], Martin Clémancey[1], Catherine Gerez[1], Yohann Duverger[2], Isabelle Kieffer[3], Frédéric Barras[4], Serge Gambarelli[5], Geneviève Blondin[1] and Sandrine Ollagnier de Choudens[1]**

1 Univ. Grenoble Alpes, CNRS, CEA, Laboratoire de Chimie et Biologie des Métaux, F-38000 Grenoble, France

2 Laboratoire de Chimie Bactérienne, UMR7243 Aix-Marseille Université CNRS, 31 Chemin Joseph Aiguier, 13009, Marseille, France

3 Univ. Grenoble Alpes, CNRS, IRD, Irstea, Météo France, OSUG, FAME, 38000 Grenoble, France

4 Institut Pasteur, Université de Paris, CNRS UMR 6047, Department of Microbiology, SAMe Unit, Paris, France

5 Univ. Grenoble Alpes, CNRS, CEA, SyMMES, F-38000 Grenoble, France

KEYWORDS

Iron-sulfur cluster; SUF pathway; XAS; Mössbauer spectroscopy; Fe-S biogenesis; Fe-S ligands; Fe-S Scaffold.

ABSTRACT

Iron-sulfur (Fe-S) clusters are essential inorganic cofactors dedicated to a wide range of biological functions including electron transfer and catalysis. Specialized multi-protein machineries present in all types of organisms support their biosynthesis. These machineries encompass a scaffold protein on which Fe-S clusters are assembled before being transferred to

cellular targets. Here, we describe the first characterization of the native Fe-S cluster of the anaerobically purified $SufBC_2D$ scaffold from *Escherichia coli* by XAS, Mössbauer, UV-visible absorption and EPR spectroscopy. Interestingly, we propose that $SufBC_2D$ harbors two iron-sulfur containing species, a [2Fe-2S] cluster and an as yet unidentified species. Using mutagenesis and biochemistry amino-acid ligands were proposed for the [2Fe-2S] cluster, supporting the hypothesis that both SufB and SufD are involved in Fe-S cluster ligation. The [2Fe-2S] cluster can be transferred to ferredoxin in agreement with $SufBC_2D$ scaffold function. These results are discussed in the context of Fe-S cluster biogenesis.

INTRODUCTION

Iron-sulfur clusters are essential protein cofactors that enable proteins to perform a variety of unique and complex functions, ranging from redox chemistry, amino-acid biosynthesis to DNA replication and repair.[1-3] These cofactors exist under different forms, [2Fe-2S], [3Fe-4S] and [4Fe-4S] being the most prevalent ones. Their biogenesis is highly regulated and conserved among organisms. Despite their significance, a number of questions still remains regarding the mechanism through which Fe-S clusters are generated. In *Escherichia coli* (*E. coli*), production of Fe-S clusters occurs via two major pathways, ISC and SUF.[4] While ISC directs Fe-S generation under normal conditions, SUF takes over during periods of iron depletion and oxidative stress. The *E. coli* SUF system consists of six proteins (SufABCDSE) among which SufB, SufC and SufD form the $SufBC_2D$ complex, which serves as a scaffold for the synthesis of nascent Fe-S clusters.[5] The cysteine desulfurase SufS uses its PLP to mobilize sulfur from L-cysteine; sulfurtransferase SufE

enhances SufS activity[6, 7] while SufA, an Fe-S carrier, transports Fe-S clusters from $SufBC_2D$ to targets.[8, 9]

The crystal structure of *E. coli* $SufBC_2D$ without Fe-S cluster was solved at 2.9 angstrom.[10] SufB interacts with both SufD and SufC, and SufD with both SufB and SufC. Thus, each SufC subunit is bound to a subunit of SufB-SufD heterodimer. After chemical reconstitution or anaerobic purification of $SufBC_2D$, the complex binds either a [2Fe-2S] or a [4Fe-4S] cluster.[5, 10-12] A bound-$FADH_2$ cofactor can also be present after anaerobic purification of the complex.[5, 11] It has been suggested for a long time that the cluster is localized on SufB subunit since, *in vitro*, SufB protein assembles after reconstitution an Fe-S cluster (either [2Fe-2S] or [4Fe-4S]) resembling that of the $SufBC_2D$ complex.[11, 13, 14] However, recent *in vivo* data (complementation assays combined with color of host cells expressing variant $SufBC_2D$) identified amino-acids both in SufB and SufD subunits which appeared to play a role for the formation and/or coordination of the Fe-S cluster within the complex[15], namely $SufB^{C405}$, $SufB^{E432}$, $SufB^{H433}$, $SufB^{E434}$, $SufD^{H360}$ and $SufD^{C358}$, supporting the notion that the Fe-S cluster is bound at the SufD-SufB interface. In order to solve this conundrum and gain insight into the true organization of the Fe-S-bound $SufBC_2D$ complex, we undertook a thorough characterization of the as-isolated *E. coli* Fe-S-$SufBC_2D$ complex using X-ray absorption, Mössbauer, UV-visible and EPR spectroscopies, combined with biochemical and mutagenesis studies. This broad and multidisciplinary approach has provided with molecular information, leading us to propose two populations of Fe-S species bound $SufBC_2D$ complexes.

RESULTS and DISCUSSION

XAS analysis of the anaerobically purified $SufBC_2D$ complex.

His_6-SufBC_2D complex was co-synthesized with SufSE from the pETDuet-1 plasmid.[11] After anaerobic purification, SEC-MALLS-RI confirmed the homogeneity of the sample with a BC_2D stoichiometry (Figure S1). The as-purified SufBC_2D complex contains an average of 2.4±0.2 Fe, 2.3±0.1 S and 0.05±0.05 $FADH_2$ per complex. It displays a brown-blackish color with an unusual UV-vis absorption spectrum: a main absorption band at 420 nm and shoulders at 320 nm, 530 nm, and 620 nm (Figure 1B). This UV-vis. spectrum is reminiscent of that described for a linear [3Fe-4S] cluster, with absorptions bands at 320, 415, 513 and 573 nm.[16-19] These results are somewhat different (Fe, S and Flavin content; complex homogeneity) to those described by Saini et al. that purified anaerobically the complex, and they might result to the different method/protocol used.

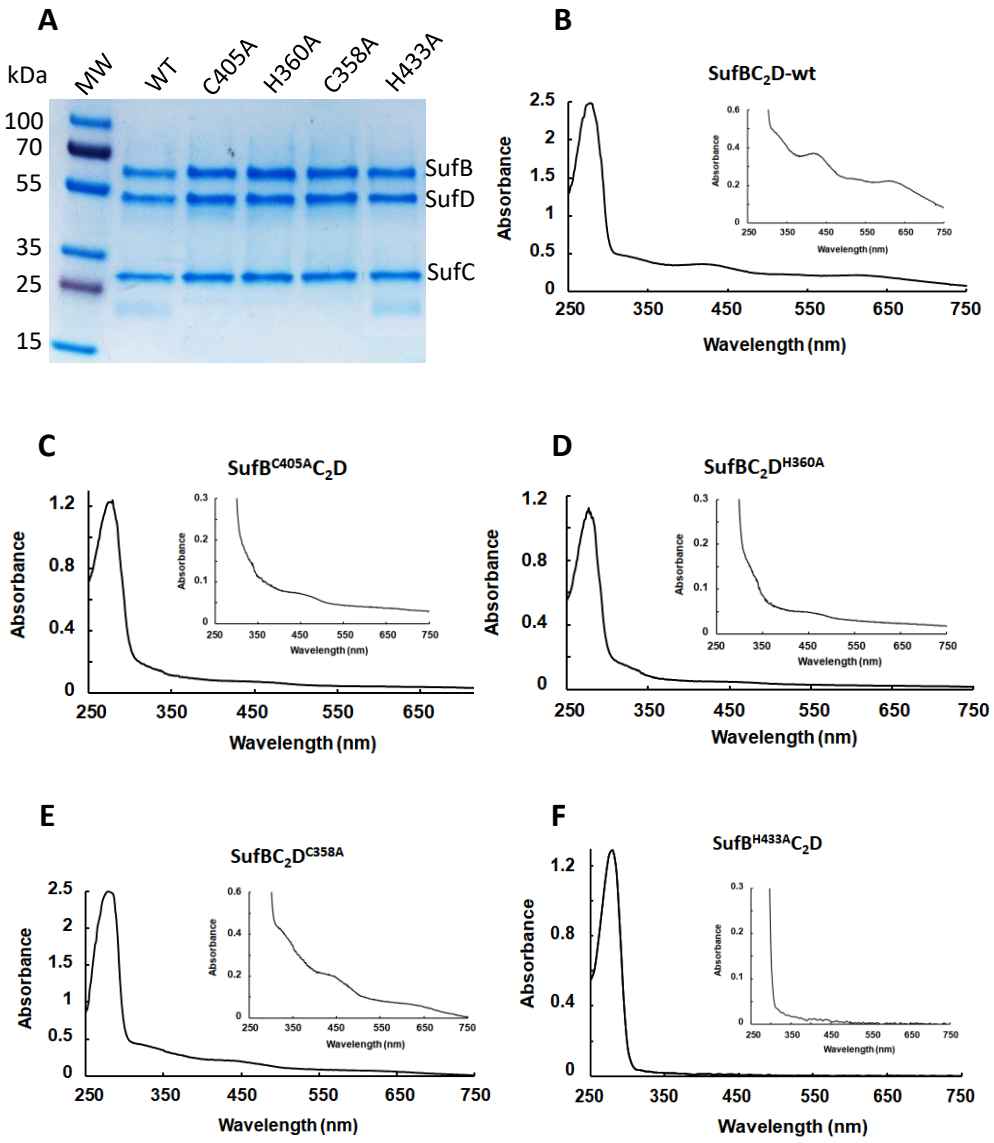

Figure 1. Anaerobic purification of SufBC$_2$D-His wild-type and variants. SDS-PAGE (A) and UV-Vis absorption spectra of anaerobically purified SufBC$_2$D-wt (B) and SufBC$_2$D variants ((C) to (F)). The *insets* of UV-vis. spectra show an enhancement of the Fe-S absorption bands. MW: Molecular weight (kDa).

This complex was therefore analyzed by X-ray absorption spectroscopy. The X-ray Absorption Near Edge Structure (XANES) spectrum of the complex (Figure 2A) exhibits all the features associated with tetrahedral Fe in Fe-S clusters, notably a prominent pre-peak at ~7113 eV, a shoulder in its rising edge at ~ 7122 eV, and a relatively featureless post-edge trend. However, from the XANES fingerprint alone we cannot discriminate between [4Fe-4S], [3Fe-4S] and [2Fe-2S], given that similar features have been observed for all kinds of clusters.[20-26] Moreover, we cannot speculate on the average oxidation state of Fe based on the energy position of the rising edge, considering that the absolute value of the latter depends on the clusters nuclearity and ligation, [21-23]

In order to determine the nature of the cluster, the Extended X-ray Absorption Near Edge Structure (EXAFS) spectrum was fitted in the range 1-3.0 Å, assuming a tetrahedral Fe environment composed of sulfur and oxygen/nitrogen ligands, and a variable number of second-shell Fe atoms (Figure 2B). In the first instance the number of ligands of each species, the relative distance, and Debye-Waller factors (σ^2) were allowed to vary. The best-fitting average Fe environment included 2.8 ± 0.3 S at 2.27 ± 0.01 Å from the absorber, 1.2 ± 0.3 N/O at 2.04 ± 0.02 Å, and 1.3 ± 0.3 Fe at 2.75 ± 0.01 Å. The σ^2 values were 4.6 ± 0.9 $\cdot 10^{-3}$Å^2, 9 ± 5 $\cdot 10^{-3}$Å^2, and 5 ± 2 $\cdot 10^{-3}$Å^2, respectively. The goodness-of-fit was R=0.6% (Figure 2B). The number of Fe around the absorber, 1.3 ± 0.3 Fe, is consistent with a [2Fe-2S] cluster or a mixture of clusters of higher nuclearity. However, we were aware that the well-known correlation between the number of atoms of a given species around the absorber and the relative Debye-Waller factor could bias the fit results. Therefore, to disentangle these parameters, we built several models with fixed numbers of neighbors according to the existing Fe-S clusters, and fitted them to the experimental data by allowing only interatomic distances and Debye-Waller factors to vary. The models

included *n* sulfur ligands and (4-*n*) oxygen/nitrogen ligands in the first shell around the absorber, and different numbers of Fe atoms in the second shell.

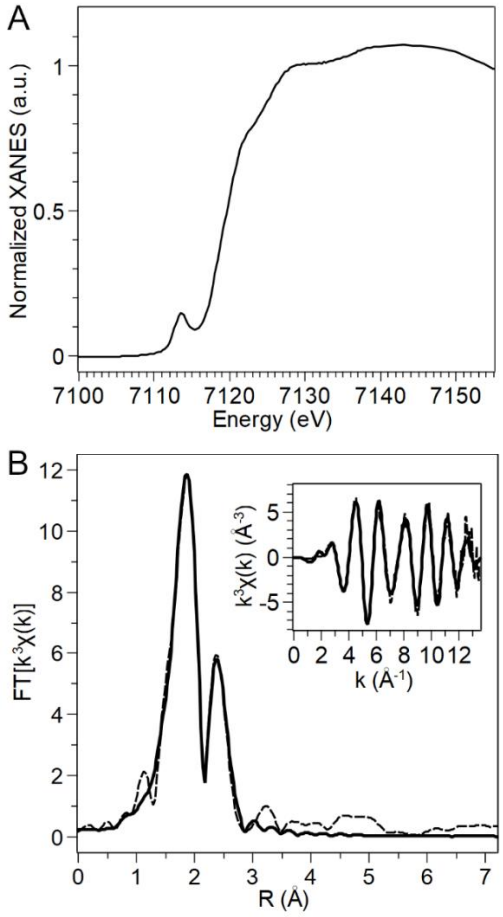

Figure 2. Fe K-edge X-ray Absorption Spectroscopy of the SufBC$_2$D complex (1.4 mM, 3.6 mM iron). (A) Experimental XANES spectrum. (B) Experimental (dashed curves) EXAFS spectrum in the reciprocal space (inset) and Fourier-transformed into the real space (main panel); relative best-fitting curve (solid curves) obtained in the real space (main panel), and back-transformed into the reciprocal space (inset).

The number of S atoms per Fe absorber, *n*, ranged from 2 (the minimum number of S ligands, encountered in a [2Fe-2S] cluster anchored to the protein through non-Cys residues) to 4 (in case the cluster was anchored to the protein only through Cys residues). Non-integer *n* values reflect a possible asymmetry between different Fe centers in the cluster. The number of second-shell Fe atoms was set to 1, 1.33, 2, or 3 to model [2Fe-2S], linear [3Fe-4S], cubane [3Fe-4S], and [4Fe-4S] clusters, respectively. This resulted in nineteen models to be fitted to the experimental data, as reported in Table 1. The possible clusters corresponding to each model are represented in Figure S2. The comparison between the goodness-of-fit (R_{fit} values in Table 1) of [2Fe-2S] models, [3Fe-4S] models and [4Fe-4S] models with the same Fe coordination sphere (e.g. model 4S 1Fe vs 4S 3Fe) systematically favored the [2Fe-2S] and linear [3Fe-4S] clusters. Moreover, in the [4Fe-4S] models, the dynamical parameter σ^2 relative to the Fe-Fe interaction was always estimated as 0.013 $Å^2$, which is very high for a metal-metal interaction, and thus probably overestimated to compensate for the excessively high value of Fe-Fe interactions in the model. In highly distorted multinuclear metal clusters, metal-metal interactions with different distances can cancel out and result in an average scattering contribution associated to a high σ^2 value, and good fit quality.[27] However, considering that in the high nuclearity models we systematically obtain a poor goodness-of-fit, we are prone to exclude the hypothesis of a highly distorted [4Fe-4S] cluster. In contrast, the [2Fe-2S] models and linear [3Fe-4S] provide the best fits, and σ^2 values between 0.003 and 0.005 $Å^2$ for the Fe-Fe interaction. These values are compatible with those provided in literature for various Fe-S cluster systems.[21, 24, 26, 28, 29]

Three models provided the best agreement with the experimental data, with a goodness-of-fit of R=0.6% (Table 1). The first was 3S 1N/O 1Fe, corresponding to a [2Fe-2S] cluster where the average Fe coordination sphere is composed of 3S and 1N/O atoms (see Figure S2).

Considering that 2 sulfur atoms belong to the inorganic sulfides bridging the metal centers, the cluster is anchored to the protein scaffold through two S and two N/O donors. The two other models, 3S 1N/O 1.33Fe and 2.67S 1.33N/O 1.33Fe correspond to linear [3Fe-4S] anchored to the protein through one S and three O/N donors, or through N/O donors only, respectively (see Figure S2). The number of Fe neighbors estimated in the initial fit, where all parameters were allowed to vary, was 1.3 ± 0.3, which is consistent with [2Fe-2S] and/or linear [3Fe-4S] cluster(s). Such geometries of Fe-S clusters are in agreement with UV-visible analyses.

Table 1. Results of ab initio fitting of the Fe K-Edge EXAFS spectrum of the SufBC$_2$D complex based on different cluster models.[a,b]

Model	number of Cys ligands	Fe-S		Fe-N/O		Fe-Fe		ΔE_0 (eV)	R_{fit} (%)
		R (Å)	σ^2 (10^3 Å^2)	R (Å)	σ^2 (10^3 Å^2)	R (Å)	σ^2 (10^3 Å^2)		
[2Fe-2S] models									
4S 1Fe	4	2.263 (12)	7.3 (9)	-	-	2.731 (18)	3 (2)	-3 (1)	2.9
3.5S 0.5O/N 1Fe	3	2.261 (12)	6.0 (9)	2.11 (7)	5[c]	2.733 (12)	3.2 (11)	-2 (1)	1.0
3S 1O/N 1Fe	2	2.271 (7)	5.1 (6)	2.05 (2)	8 (5)	2.744 (9)	3.2 (9)	-0.5 (8)	**0.6**
2.5S 1.5O/N 1Fe	1	2.281 (7)	3.9 (6)	2.03 (3)	9 (3)	2.753 (10)	3.3 (10)	1.2 (9)	0.9
2S 2O/N 1Fe	0	2.289 (11)	2.8 (9)	2.03 (2)	8 (3)	2.762 (15)	3.6 (16)	3 (1)	1.8
linear [3Fe-4S] models									
4S 1.33Fe	4	2.262 (13)	7.1 (9)	-	-	2.736 (18)	5 (2)	-3 (1)	3.4
3.67S 0.33O/N 1.33 Fe	3	2.260 (11)	6.1 (20)	2.16 (30)	5[c]	2.733 (20)	5.2 (16)	-3 (2)	1.5
3.33S 0.67O/N 1.33 Fe	2	2.262 (8)	5.6 (11)	2.09 (7)	8 (14)	2.738 (13)	5.2 (11)	-2 (1)	0.9
3S 1O/N 1.33Fe	1	2.269 (6)	5.0 (6)	2.05 (12)	9 (6)	2.745 (9)	5.1 (9)	-0.8 (8)	**0.6**
2.67S 1.33O/N 1.33Fe	0	2.275 (6)	4.2 (5)	2.03 (1)	10 (4)	2.751 (9)	5.2 (9)	0.3 (7)	**0.6**
cubane [3Fe-4S] models									
4S 2Fe	3	2.261 (15)	6.8 (9)	-	-	2.74 (2)	8 (3)	-3 (1)	4.9
3.67S 0.33O/N 2Fe	2	2.259 (11)	6 (3)	2.2 (5)	5[c]	2.74 (3)	9 (2)	-3 (2)	2.5
3.33S 0.67O/N 2Fe	1	2.259 (11)	5.5 (8)	2.11 (6)	5[c]	2.741 (14)	8.7 (15)	-2 (1)	1.8
3S 1O/N 2Fe	0	2.265 (8)	4.7 (7)	2.06 (3)	12 (10)	2.745 (12)	8.7 (12)	-1 (1)	1.2
[4Fe-4S] models									
4S 3Fe	4	2.259 (18)	6.5 (10)	-	-	2.74 (3)	13 (4)	-3 (2)	7.0
3.75S 0.25O/N 3Fe	3	2.260 (17)	6.2 (8)	2.05[c]	5[c]	2.74 (2)	13 (3)	-3 (2)	5.3

3.5S 0.5O/N 3Fe	2	2.256 (12)	5 (3)	2.2 (4)	5[c]	2.74 (3)	13 (2)	-3(3)	3.3
3.25S 0.75O/N 3Fe	1	2.254 (14)	5 (2)	2.15 (16)	5[c]	2.74 (3)	13 (2)	-3 (2)	2.9
3S 1O/N 3Fe	0	2.262 (13)	4.5 (10)	2.08 (7)	15 (20)	2.744 (2)	13 (2)	-1 (2)	2.4

[a]Fixed parameters: numbers of S, O/N, and Fe atoms. The Debye-Waller factors were fitted starting from values comparable with the ones found in the literature for different [Fe-S] clusters: σ^2(Fe-S) = 0.003 Å^2, σ^2(Fe-Fe) = 0.003 Å^2, σ^2(Fe-O) = 0.005 Å^2. [b]R, interatomic distance; σ^2, Debye Waller factor; ΔE_0, shift in the energy origin; R_{fit}, goodness-of-fit calculated as $\Sigma(x_{exp}-x_{fit})^2/\Sigma(x_{exp})^2$, where x_{exp} is the experimental data point, and x_{fit} the corresponding point in the best-fitting curve. The error on the last digit is reported in parenthesis. [c]This value was fixed during the fit. In bold are the favored models.

Mössbauer and EPR spectroscopies of the anaerobically purified SufBC$_2$D complex

We then turned to EPR and Mössbauer spectroscopy to identify/ or further characterize the Fe-S clusters of the as-isolated SufBC$_2$D complex. We used for both spectroscopy the anaerobically purified ^{57}FeS-SufBC$_2$D sample that corresponded to as-isolated SufBC$_2$D expressed in the presence of ^{57}Fe in culture medium and purified under anaerobic conditions. After purification, the ^{57}FeS-SufBC$_2$D sample contained the same iron, sulfur and flavin content (average of 2.4±0.3 Fe, 2.3±0.1 S and 0.04±0.04 $FADH_2$ per complex) and presented the same UV-vis. spectrum as those of the ^{56}FeS-SufBC$_2$D sample (Figure 1B). By EPR spectroscopy, no intense signal was detected, whatever the conditions used (low/high temperature, power, modes (parallel vs perpendicular)) (Figure S3). In perpendicular mode, the low-field spectrum recorded at low temperature (5 K) and high power (10 mW) consisted only of a very small signal at g=4.3 (Figure S3A). This signal likely corresponds to adventitiously-bound high-spin (S=5/2) Fe^{3+} species. No significant signal was visible at lower fields (Figure S3A), in particular around g=9.6, where additional features are usually detected in the spectrum of linear [3Fe-4S]$^{1+}$.[16, 18, 19] Comparison with a known sample containing a linear [3Fe-4S]$^{1+}$ cluster revealed a maximum possible concentration of 7.2 µM (Table 2 and Figure S4B). This corresponds to 5.3 % of iron

versus the total iron content. Once again in perpendicular mode, but at a higher temperature (20 K) and lower power (1 mW), accumulation allowed us to observe a signal at g=2.01 (Figure S3B). This signal may correspond to a cubane [3Fe-4S]$^{1+}$ cluster or to a semiquinone radical (FADH$^{\bullet}$) resulting from semi-oxidation of $FADH_2$. The very low intensity of this signal made further characterization impossible. Even though this signal at g=2.01 does correspond to that expected for an oxidized cubane [3Fe-4S]$^{1+}$ cluster, the absolute quantification indicates a maximum possible concentration of 5.6 µM (Figure S4A and Table 2), that would then account for 4.1% of iron versus the total iron content. In parallel mode, no signal was detected, even after extensive temperature/power optimization (Figure S3C). Taken together, these EPR spectroscopy results allow to rule out the presence of classical all-ferric [3Fe-4S] clusters, whatever the linear or cubane geometry. These results suggest the presence of diamagnetic or integer spin iron-based clusters (the lack of signal in the parallel mode low frequency EPR cannot be taken as evidence of the lack of integer spin species). However, a half-integer spin species with large distribution and weak ZFS (zero-field splitting) parameters cannot be excluded.

Table 2. EPR and Mössbauer spectroscopy analysis of SufBC$_2$D complex. SufBC$_2$D concentration for EPR spectroscopy (150 µM, 2.7 iron/complex) and Mössbauer (290 µM, 2.7 iron/ complex). *****Absolute quantification of signals by EPR spectroscopy was performed using reference samples described in the experimental part. (-) : not identified

		Mössbauer spectroscopy Sample at 290 µM	**EPR spectroscopy***	**EPR spectroscopy Sample at 150 µM**
Electronic Spin	**Type of species**	% of Fe (vs total iron)	µM of spin	% of Fe (vs total iron)
	[2Fe-2S]$^{2+}$	35	Not responsive	-

S=0	**[4Fe-4S]$^{2+}$**	0	Not responsive	-
S=1/2	**Radical FADH°**	Not responsive	5.6	0
	[2Fe-2S]$^{1+}$	-		2.8
	Cubane [3Fe-4S]$^{1+}$	-		4.1
	[4Fe-4S]$^{1+}$	-		5.5
S=2	**Cubane [3Fe-4S]^{0}**	0	0	0
S=5/2	**Linear [3Fe-4S]$^{1+}$**	0	7.2	5.3
S= integer or half integer	**Unknown**	65	-	-

To identify these EPR-silent species within the as-isolated SufBC$_2$D complex, we performed Mössbauer spectroscopy. Mössbauer spectroscopy on three samples returned identical results. Firstly, a Mössbauer spectrumwas recorded at high temperature ca. 230 K in a 60 mT external magnetic field applied parallel to the gamma rays to detect doublets associated to different types of iron sites. This spectrum revealed the superposition of two quadrupole doublets (Figure 3a). The parameters of the main doublet (89%, δ = 0.23 mm/s, ΔE_Q = 0.52 mm/s) are consistent with Fe^{3+} ions (S=5/2) in a tetrahedral geometry (Figure 3a, in blue). The minority doublet (11%, δ = 0.48 mm/s, ΔE_Q = 1.00 mm/s) has an isomer shift parameter value that lies between those corresponding to Fe^{2+} and $Fe^{2.5+}$ ions (Figure 3a, in purple).[30]

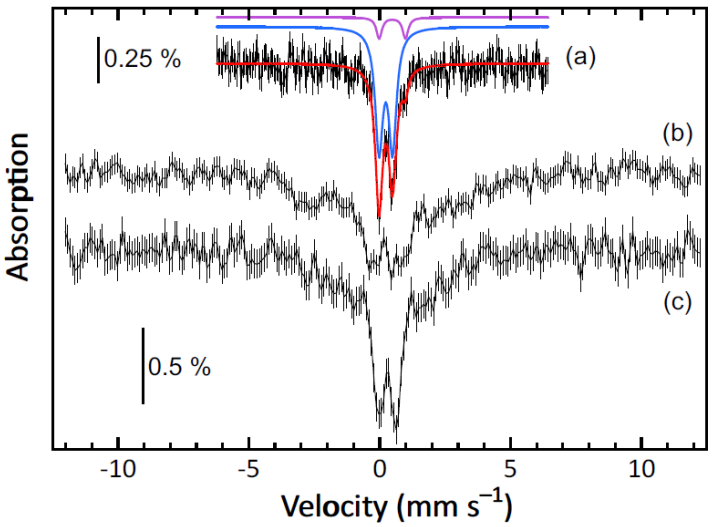

Figure 3: **Experimental Mössbauer spectra of SufBC$_2$D complex. (a) Spectrum** recorded at ca 230 K with a 0.06 T external magnetic field applied parallel to the γ-rays direction (vertical bars, SufBC$_2$D: 290 µM, 2.6 Fe/complex). A simulation is overlaid (solid red line) and the two contributions displayed above as colored traces. See text for parameters. (b-c) Spectra recorded at 6 K with a 0.06 (c) and 4 T (b) external magnetic field applied parallel to the γ-rays direction (vertical bars, SufBC$_2$D: 290 µM, 2.7 Fe/complex).

Secondly, spectra at helium temperature were recorded using external magnetic field with different strengths in order to access the electronic structure of the iron sites. At 6 K in a 60 mT external magnetic field applied parallel to the gamma rays, the Mössbauer spectrum presents absorption between -2 mm/s and +3 mm/s (Figure 3c). The two lines observed in the central part can be assigned to a doublet originating from a first species. This doublet can be reproduced with nuclear parameters (δ = 0.30 mm/s, ΔE_Q = 0.63 mm/s) that are consistent with a diamagnetic [2Fe-2S]$^{2+}$ cluster with ferric sites coordinated with sulfur and oxygen/nitrogen atoms (see Figure S5).

The presence of a [2Fe-2S] cluster in SufBC$_2$D was confirmed by Fe-S cluster transfer experiments to *E. coli* ferredoxin (a [2Fe-2S] protein) and to *E. coli* aconitase B (a [4Fe-4S] enzyme). In the latter case, the transfer was only observed in the presence of a reducing agent which is required to allow the reductive coupling of two $[2Fe\text{-}2S]^{2+}$ clusters to a $[4Fe\text{-}4S]^{2+}$ cluster (Figure S6)[8]. The low-temperature Mössbauer spectrum (6 K in a 60 mT magnetic field) also displays a broad additional absorption suggesting the presence of a second species (Figure 3c and S5A). To better characterize this system, a Mössbauer spectrum was recorded at 6 K using a 4 T magnetic field applied parallel to the γ-rays (Figure 3b). This field magnitude was chosen to evidence linear $[3Fe\text{-}4S]^{1+}$ clusters, an arrangement of the Fe-S cluster of SufBC$_2$D deduced from the X-absorption analysis. Such clusters, exhibiting a S=5/2 ground state, usually present intense absorption lines at –4.5 and +5 mm/s.[16, 18] These lines were not detected, which is fully consistent with EPR studies. Moreover, the lack of defined absorption lines, made it impossible to determine the magnetic species present alongside the oxidized [2Fe-2S] cluster. A 35% upper limit in terms of iron content can be estimated for the [2Fe-2S] cluster that accounts for at most 44% of the SufBC$_2$D complex population (Table 2). The second magnetic species therefore accounts for 65% in terms of iron concentration, and 56% of the SufBC$_2$D complex population (Table 2). The persistency at zero-field (Figure S7) of the magnetic contribution allows to rule out the presence of $[3Fe\text{-}4S]^{0}$, all reduced cubane clusters presenting a S=2 ground state that is characterized by doublets in these recording conditions.[31] This is also sustained by the comparison of the experimental data with the magnetic spectra typically observed for $[3Fe\text{-}4S]^{0}$ clusters (see Figure S8). Cuboidal S=1/2 $[3Fe\text{-}4S]^{1+}$ clusters[32] is a more attractive possibility (see Figure S9C and D) but hardly compatible with the weak perpendicular mode X-band EPR signal observed in the g=2 region.

To shed light on the species that could exist in the as-purified $SufBC_2D$ sample, we attempted to reduce the sample with dithionite. UV-visible absorption spectroscopy indicated that the sample had effectively been reduced (inset Figure S3D). Analysis of the reduced sample by EPR spectroscopy revealed only the cavity signal (Figure S3D). Thus, this experiment did not allow to detect reduced [2Fe-2S] nor to attribute the second iron species present in the sample. It is likely that reduction destroyed the [2Fe-2S] cluster and the other sulfur iron-containing species, since re-oxidization with air did not allow the sample to recover its pre-reduction absorption profile. The irreversibility of the reduction reaction also excludes the possibility that some sort of cluster conversion reaction could have occurred during reduction.

Altogether, EPR and Mössbauer spectroscopies suggest that the $SufBC_2D$ complex exists in two possible types. One type – accounting for at most ~44% of the $SufBC_2D$ complex population –binds a $[2Fe\text{-}2S]^{2+}$ cluster (this corresponds to the maximum 35% versus the total iron content associated with [2Fe-2S] clusters). The other type – accounting for ~56% of the population binds an iron-containing species that can be either a half-integer spin species presenting a Kramers doublet as the ground state but with ZFS parameters precluding an EPR signal, or an integer spin species presenting a nearly degenerate doublet that would be EPR silent.

Recalling that biochemical analysis indicated an average Fe content of 2.4 ± 0.2 per complex (and 2.3 ± 0.1 S), we are prone to consider that in this second species Fe has a nuclearity higher than 2. We can also recall that the EXAFS analysis indicated an average Fe coordination as in a [2Fe-2S] cluster or in a linear [3Fe-4S] cluster (values per Fe absorber: 2.8 ± 0.3 S, 1.2 ± 0.3 N/O and 1.3 ± 0.3 Fe). In the light of the presence of two species, only one of which is a [2Fe-2S] cluster, we expect a nuclearity higher than 2 for the second species. We propose that these two $SufBC_2D$ populations coexist, at least in the conditions used in our study.

Mutagenesis analysis of the SufBC$_2$D complex.

A previous study carried out *in vivo* on *E. coli* proposed SufB Cys405, Glu432, His433 and Glu434 residues, as well as SufD Cys358 and His360 residues to be functionally important residues for Fe-S formation. This study alone is not sufficient to pinpoint the Fe-S coordination.[15] Indeed, Glu434 and Glu432 point in the opposite direction of the other important residues for Fe-S assembly (Cys405, His433, Cys358 and His360) (Figure S10). Glu434 is a conserved amino-acid in SufB proteins whereas Glu432 is not (Figure S11). Cys358 in SufD proteins is not strictly conserved either (Figure S11), but it is one of the mercuric ion ligands in the Hg^{2+}-containing SufBC$_2$D structure (PDB: 5AWG). Having been able to obtain the purified wild-type SufBC$_2$D complex with a [2Fe-2S] cluster, we decided to proceed identically with variants of the complex to obtain molecular information on the cluster's ligands.[10] Therefore, we constructed SufB^{C405A}CD, SufB^{H433A}CD, SufB^{E434A}CD, SufBCD^{C358A} and SufBCD^{H360A} variants and assessed their role in cluster binding by analyzing UV-vis. absorption spectra and the iron/sulfur content of anaerobically purified variant complexes. With the exception of the SufB^{E434A}CD variant (Figure S12A-B), SDS-PAGE of variant complexes indicates that they contain the three proteins SufB, SufC and SufD, as observed for the wild-type complex (Figure 1A). Whereas these four mutations had little or no effect on complex formation, distinctive UV-vis. signatures were observed (Figure 1C-1F). Moreover, as detailed below, the Fe and S contents were all significantly lower than those of the wild-type (2.4 Fe and 2.3 S/complex) (Figure 1B). The UV-visible spectra of the SufB^{C405A}C$_2$D and SufB^{H433A}C$_2$D variants display little, if any, absorption at 420 nm, and they have a very poor iron binding capacity (0.1 Fe and 0.1 S/complex) (Figure 1C and 1F). The SufBC$_2$D^{H360A} variant is also affected in its Fe-S assembly as shown by the low absorption bands

in the 320-500 nm region, and the low Fe and S content: 0.4 Fe and 0.3 S/complex (Figure 1D). Although the UV-vis. spectrum of $SufBC_2D^{C358A}$ displays low absorption bands, the iron and sulfur content of this complex (1.3 Fe and 1.5 S/complex) suggests that this variant can still bind an Fe-S cluster (Figure 1E). Surprisingly, as mentioned above, we were unable to isolate the $SufB^{E434A}C_2D$ complex suggesting, in contrast to previous reports[15], that the mutation E434A in SufB has a drastic destabilizing effect (Figure S12A-B). In contrast, we were able to purify the $SufB^{E434K}C_2D$ and the $SufB^{E434D}C_2D$ variants. Both displayed low absorption bands on their respective UV-vis. absorption spectrum (Figure S12C-D) and poor levels of iron and sulfur (0.3 Fe and S/complex for $SufB^{E434K}C_2D$; 0.55 Fe and 0.5 S/complex for $SufB^{E434D}C_2D$), indicating that this Glu434 residue is important for Fe-S assembly. Altogether, these data obtained on purified complexes strongly suggest that Cys405, His433 and Glu434 from SufB as well as Cys358 and His360 from SufD are involved in Fe-S cluster ligation/assembly of the *E. coli* $SufBC_2D$ complex.

Based on these results, we propose the [2Fe-2S] cluster to be coordinated by SufB residues Cys405 and His433 and SufD residues Cys358 and His360, in line with the XAS data predicting 1 O/N neighboring atom per Fe. The XAS results are also compatible with the Glu434 residue acting as a ligand (via an oxygen atom on its side chain) of [2Fe-2S]. However, this seems unlikely because the side chain of this residue is positioned in the opposite direction to that of the other predicted ligands (notably cysteines Cys405 and Cys358) (Figure S10). Rather than participating in cluster coordination, the glutamate residue could be involved in cluster building or transfer. The sulfur coordination provided by Cys405 and Cys358 in the [2Fe-2S] cluster is consistent with the crystallographic structure of Hg^{2+}-containing $SufBC_2D$ complex in which the two Hg^{2+} ions are bound to Cys405 (in SufB) and Cys358 (in SufD) (PDB: 5AWG).[10] The Cys405 residue is strictly conserved throughout SufB proteins in prokaryotes, including eubacteria, archaea and plants

(Figure S11). In contrast, SufD Cys358 is not conserved in firmicutes such as *Bacillus subtilis* (Figure S11). However, the *E. coli* and *B. subtilis* SUF systems show a series of differences from genetic organization to genetic composition, and were recently demonstrated to exhibit distinct efficiencies in maturing heterologous Fe-S targets[33, 34]. In contrast, both SufB His433 and SufD His360 – which we propose to serve as nitrogen ligands – are strictly conserved (Figure S11). Moreover, we propose that these residues each coordinates a different Fe atom in the [2Fe-2S] cluster. The isomer shift obtained for the iron sites of the proposed [2Fe-2S] cluster in SufBC$_2$D is consistent with that observed for ferric sites with 1 Cys and 1 His, as observed for one of the iron sites in IscR[35] or MitoNEET[36], rather than with that determined for Rieske type proteins[37] or Apd1 [38], where the iron site is coordinated by 2 His (Table S1). Therefore, we propose (based on our Mössbauer, EXAFS and mutagenesis data) that the iron sites of the [2Fe-2S] cluster in SufBC$_2$D are coordinated by two SufB residues, namely Cys405 and His433, and two SufD residues, namely Cys358 and His360 (Figure 4). This coordination mode would be similar to that found in RsrR, where one Fe^{3+} is coordinated by 1 Cys and 1 His and the other by 1 Cys and 1 Glu. [39, 40] The fact that no flavin are present in our sample that contains Fe-S clusters, may suggest that the Flavin is involved during the Fe-S assembly mechanism even though this has to be demonstrated.

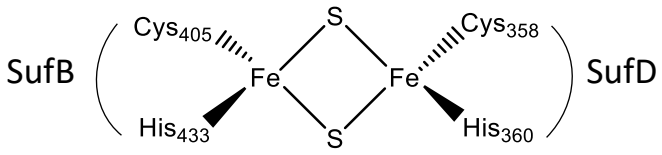

Figure 4: Proposed coordination of SufBC$_2$D [2Fe-2S] cluster.

Conclusion: In this work, we have presented the first XAS spectrum of the anaerobically purified SufBC$_2$D scaffold from *E. coli*, as well as its Mössbauer, UV-vis. and EPR analysis. These spectroscopic techniques allowed us to identify two populations of SufBC$_2$D complex, one containing a [2Fe-2S] and one harboring an unidentified species. The detailed biochemical characterization on purified wt and variant SufBC$_2$D complexes allowed us to propose residues from SufB and SufD acting as ligands for the [2Fe-2S] cluster. Our results reveal that the as-isolated SufBC$_2$D complex, containing a [2Fe-2S] cluster, can transfer its cluster to apo-ferredoxin, in agreement with its scaffold function. The current accepted view is that bacterial IscU and SufBC$_2$D behave like scaffolds, assembling a [2Fe-2S] cluster that is subsequently transferred to A-type proteins, where it can be converted to [4Fe-4S] (via a reductive coupling) for targeting to apo-targets.[41-47] It should be noted, however, that A-type proteins are also instrumental in the maturation of [2Fe-2S]-containing proteins such as IscR or SoxR in *E. coli*.[48, 49] The observation of a [2Fe-2S] cluster on as-purified SufBC$_2$D is in agreement with this view.

The existence of a second unknown species in SufBC$_2$D was reproducible over several replicates, and is unlikely to be an artifact. However, the question of its physiological relevance remains. One can also speculate that it may correspond as an intermediate in the Fe-S cluster formation. Even though we do not favor this hypothesis, it can be also a degradation product of higher nuclear Fe-S species such as [4Fe-4S] cluster. The evidence for the existence of this species, although currently obscure, is completely fascinating in the context of Fe-S assembly and more broadly in the field of bioinorganic chemistry. Identification of this species must be considered as a new challenge to the community as well as the identification of the Flavin role.[50]

ASSOCIATED CONTENT

Supporting information: Materials and methods; Additional results of experiments (SEC-MALLS-RI, EPR and Mössbauer spectra of $SufBC_2D$ complex, Biochemical properties of $SufB^{E434A}C_2D$, $SufB^{E434K}C_2D$ and $SufB^{E434D}C_2D$ variants, Fe-S cluster transfer experiments; Sequence alignments of SufB and SufD proteins); Graphical representation of the Fe-S clusters associated with models used to fit EXAFS spectrum; Structure (zoom) of the apo-$SufBC_2D$ complex (PDB 5AWF).

AUTHOR INFORMATION

Corresponding Authors

***Giulia Veronesi.** Univ. Grenoble Alpes, CNRS, CEA, Laboratoire de Chimie et Biologie des Métaux, F-38000 Grenoble, France; https://orcid.org/0000-0001-9228-6082; Email: giulia.veronesi@cea.fr

* **Sandrine Ollagnier de Choudens**. Univ. Grenoble Alpes, CNRS, CEA, Laboratoire de Chimie et Biologie des Métaux, F-38000 Grenoble, France; https://orcid.org/0000-0002-0080-6659; Email: sollagnier@cea.fr

Notes

The Authors declare no competing financial interest.

ACKNOWLEDGMENT

This work was supported by grants from Agence Nationale Recherche (ANR) ANR FeStreS (ANR-11-BSV3-022-01), the LabEx ARCANE (ANR-11-LABX-0003-01) and the CBH-EUR-GS (ANR-17-EURE-0003). We acknowledge the European Synchrotron Radiation Facility for provision of synchrotron radiation facilities (project LS-2814 on beamline BM30). We thank Tu-Quynh Nguyen and Yvain Nicolet (CEA, CNRS, IBS, Grenoble, France) and Bénédicte Burlat (Aix Marseille University, CNRS, BIP, Marseille, France) for providing us standard samples for absolute quantification in EPR analyses. Financial support from the IR INFRANALYTICS FR2054 for conducting the research is also gratefully acknowledged.

ABBREVIATIONS

Fe-S: Iron-Sulfur; XAS: X-ray Absorption Spectroscopy; EPR: Electronic Paramagnetic Resonance; UV-vis.: Ultra-Violet Visible; SEC-MALLS-RI: Size Exclusion Chromatography-Multi Angle Light Scattering-Refractive Index; DTT: dithiothreitol.

REFERENCES

1. Fuss, J. O.; Tsai, C. L.; Ishida, J. P.; Tainer, J. A., Emerging critical roles of Fe-S clusters in DNA replication and repair. *Biochim Biophys Acta* **2015,** *1853* (6), 1253-71.
2. Roche, B.; Aussel, L.; Ezraty, B.; Mandin, P.; Py, B.; Barras, F., Iron/sulfur proteins biogenesis in prokaryotes: formation, regulation and diversity. *Biochim Biophys Acta* **2013,** *1827* (3), 455-69.
3. Braymer, J. J.; Lill, R., Iron-sulfur cluster biogenesis and trafficking in mitochondria. *J Biol Chem* **2017,** *292* (31), 12754-12763.

4. Roche, B.; Aussel, L.; Ezraty, B.; Mandin, P.; Py, B.; Barras, F., Reprint of: Iron/sulfur proteins biogenesis in prokaryotes: formation, regulation and diversity. *Biochim Biophys Acta* **2013,** *1827* (8-9), 923-37.
5. Wollers, S.; Layer, G.; Garcia-Serres, R.; Signor, L.; Clemancey, M.; Latour, J. M.; Fontecave, M.; Ollagnier de Choudens, S., Iron-sulfur (Fe-S) cluster assembly: the SufBCD complex is a new type of Fe-S scaffold with a flavin redox cofactor. *J Biol Chem* **2010,** *285* (30), 23331-41.
6. Outten, F. W.; Wood, M. J.; Munoz, F. M.; Storz, G., The SufE protein and the SufBCD complex enhance SufS cysteine desulfurase activity as part of a sulfur transfer pathway for Fe-S cluster assembly in Escherichia coli. *J Biol Chem* **2003,** *278* (46), 45713-9.
7. Loiseau, L.; Ollagnier-de-Choudens, S.; Nachin, L.; Fontecave, M.; Barras, F., Biogenesis of Fe-S cluster by the bacterial Suf system: SufS and SufE form a new type of cysteine desulfurase. *J Biol Chem* **2003,** *278* (40), 38352-9.
8. Gupta, V.; Sendra, M.; Naik, S. G.; Chahal, H. K.; Huynh, B. H.; Outten, F. W.; Fontecave, M.; Ollagnier de Choudens, S., Native Escherichia coli SufA, coexpressed with SufBCDSE, purifies as a [2Fe-2S] protein and acts as an Fe-S transporter to Fe-S target enzymes. *J Am Chem Soc* **2009,** *131* (17), 6149-53.
9. Chahal, H. K.; Outten, F. W., Separate FeS scaffold and carrier functions for SufB(2)C(2) and SufA during in vitro maturation of [2Fe2S] Fdx. *J Inorg Biochem* **2012,** *116*, 126-34.
10. Hirabayashi, K.; Yuda, E.; Tanaka, N.; Katayama, S.; Iwasaki, K.; Matsumoto, T.; Kurisu, G.; Outten, F. W.; Fukuyama, K.; Takahashi, Y.; Wada, K., Functional Dynamics Revealed by the Structure of the SufBCD Complex, a Novel ATP-binding Cassette (ABC) Protein That Serves as a Scaffold for Iron-Sulfur Cluster Biogenesis. *J Biol Chem* **2015,** *290* (50), 29717-31.
11. Saini, A.; Mapolelo, D. T.; Chahal, H. K.; Johnson, M. K.; Outten, F. W., SufD and SufC ATPase activity are required for iron acquisition during in vivo Fe-S cluster formation on SufB. *Biochemistry* **2010,** *49* (43), 9402-12.
12. Chahal, H. K.; Dai, Y.; Saini, A.; Ayala-Castro, C.; Outten, F. W., The SufBCD Fe-S scaffold complex interacts with SufA for Fe-S cluster transfer. *Biochemistry* **2009,** *48* (44), 10644-53.
13. Layer, G.; Gaddam, S. A.; Ayala-Castro, C. N.; Ollagnier-de Choudens, S.; Lascoux, D.; Fontecave, M.; Outten, F. W., SufE transfers sulfur from SufS to SufB for iron-sulfur cluster assembly. *J Biol Chem* **2007,** *282* (18), 13342-50.
14. Blanc, B.; Clemancey, M.; Latour, J. M.; Fontecave, M.; Ollagnier de Choudens, S., Molecular investigation of iron-sulfur cluster assembly scaffolds under stress. *Biochemistry* **2014,** *53* (50), 7867-9.
15. Yuda, E.; Tanaka, N.; Fujishiro, T.; Yokoyama, N.; Hirabayashi, K.; Fukuyama, K.; Wada, K.; Takahashi, Y., Mapping the key residues of SufB and SufD essential for biosynthesis of iron-sulfur clusters. *Sci Rep* **2017,** *7* (1), 9387.
16. Kennedy, M. C.; Kent, T. A.; Emptage, M.; Merkle, H.; Beinert, H.; Munck, E., Evidence for the formation of a linear [3Fe-4S] cluster in partially unfolded aconitase. *J Biol Chem* **1984,** *259* (23), 14463-71.
17. Jones, K.; Gomes, C. M.; Huber, H.; Teixeira, M.; Wittung-Stafshede, P., Formation of a linear [3Fe-4S] cluster in a seven-iron ferredoxin triggered by polypeptide unfolding. *Journal of Biological Inorganic Chemistry* **2002,** *7* (4-5), 357-362.

18. Zhang, B.; Bandyopadhyay, S.; Shakamuri, P.; Naik, S. G.; Huynh, B. H.; Couturier, J.; Rouhier, N.; Johnson, M. K., Monothiol glutaredoxins can bind linear [Fe3S4]+ and [Fe4S4]2+ clusters in addition to [Fe2S2]2+ clusters: spectroscopic characterization and functional implications. *J Am Chem Soc* **2013,** *135* (40), 15153-64.
19. Villalta, A.; Srour, B.; Lartigue, A.; Clemancey, M.; Byrne, D.; Chaspoul, F.; Loquet, A.; Guigliarelli, B.; Blondin, G.; Abergel, C.; Burlat, B., Evidence for [2Fe-2S](2+) and Linear [3Fe-4S](1+) Clusters in a Unique Family of Glycine/Cysteine-Rich Fe-S Proteins from Megavirinae Giant Viruses. *J Am Chem Soc* **2023,** *145* (5), 2733-2738.
20. Musgrave, K. B.; Angove, H. C.; Burgess, B. K.; Hedman, B.; Hodgson, K. O., All-ferrous titanium(III) citrate reduced Fe protein of nitrogenase: An XAS study of electronic and metrical structure. *Journal of the American Chemical Society* **1998,** *120* (21), 5325-5326.
21. Kounosu, A.; Li, Z. R.; Cosper, N. J.; Shokes, J. E.; Scott, R. A.; Imai, T.; Urushiyama, A.; Iwasaki, T., Engineering a three-cysteine, one-histidine ligand environment into a new hyperthermophilic archaeal Rieske-type [2Fe-2S] ferredoxin from Sulfolobus solfataricus. *Journal of Biological Chemistry* **2004,** *279* (13), 12519-12528.
22. Kowalska, J.; DeBeer, S., The role of X-ray spectroscopy in understanding the geometric and electronic structure of nitrogenase. *Bba-Mol Cell Res* **2015,** *1853* (6), 1406-1415.
23. Kowalska, J. K.; Hahn, A. W.; Albers, A.; Schiewer, C. E.; Bjornsson, R.; Lima, F. A.; Meyer, F.; DeBeer, S., X-ray Absorption and Emission Spectroscopic Studies of [L2Fe2S2](n) Model Complexes: Implications for the Experimental Evaluation of Redox States in Iron-Sulfur Clusters. *Inorganic Chemistry* **2016,** *55* (9), 4485-4497.
24. Bhave, D. P.; Han, W. G.; Pazicni, S.; Penner-Hahn, J. E.; Carroll, K. S.; Noodleman, L., Geometric and Electrostatic Study of the [4Fe-4S] Cluster of Adenosine-5 '-Phosphosulfate Reductase from Broken Symmetry Density Functional Calculations and Extended X-ray Absorption Fine Structure Spectroscopy. *Inorganic Chemistry* **2011,** *50* (14), 6610-6625.
25. Hsueh, K. L.; Yu, L. K.; Chen, Y. H.; Cheng, Y. H.; Hsieh, Y. C.; Ke, S. C.; Hung, K. W.; Chen, C. J.; Huang, T. H., FeoC from Klebsiella pneumoniae Contains a [4Fe-4S] Cluster. *Journal of bacteriology* **2013,** *195* (20), 4726-4734.
26. Vaccaro, B. J.; Clarkson, S. M.; Holden, J. F.; Lee, D. W.; Wu, C. H.; Poole, F. L.; Cotelesage, J. J. H.; Hackett, M. J.; Mohebbi, S.; Sun, J. C.; Li, H. L.; Johnson, M. K.; George, G. N.; Adams, M. W. W., Biological iron-sulfur storage in a thioferrate-protein nanoparticle. *Nature Communications* **2017,** *8*, 16110.
27. Gu, W.; Seravalli, J.; Ragsdale, S. W.; Cramer, S. P., CO-induced structural rearrangement of the C cluster in Carboxydothermus hydrogenoformans CO dehydrogenase-evidence from Ni K-edge X-ray absorption spectroscopy. *Biochemistry* **2004,** *43* (28), 9029-35.
28. Cosper, N. J.; Eby, D. M.; Kounosu, A.; Kurosawa, N.; Neidle, E. L.; Kurtz, D. M.; Iwasaki, T.; Scott, R. A., Redox-dependent structural changes in archaeal and bacterial Rieske-type [Ne-2S] clusters. *Protein Science* **2002,** *11* (12), 2969-2973.
29. Blank, M. A.; Lee, C. C.; Hu, Y.; Hodgson, K. O.; Hedman, B.; Ribbe, M. W., Structural models of the [Fe4S4] clusters of homologous nitrogenase Fe proteins. *Inorg Chem* **2011,** *50* (15), 7123-8.
30. Wu, C. H.; Jiang, W.; Krebs, C.; Stubbe, J., YfaE, a ferredoxin involved in diferric-tyrosyl radical maintenance in Escherichia coli ribonucleotide reductase. *Biochemistry* **2007,** *46* (41), 11577-88.
31. Hanzelmann, P.; Hernandez, H. L.; Menzel, C.; Garcia-Serres, R.; Huynh, B. H.; Johnson, M. K.; Mendel, R. R.; Schindelin, H., Characterization of MOCS1A, an oxygen-sensitive

iron-sulfur protein involved in human molybdenum cofactor biosynthesis. *J Biol Chem* **2004,** *279* (33), 34721-32.
32. Krebs, C.; Henshaw, T. F.; Cheek, J.; Huynh, B. H.; Broderick, J. B., Conversion of 3Fe-4S to 4Fe-4S clusters in native pyruvate formate-lyase activating enzyme: Mossbauer characterization and implications for mechanism. *Journal of the American Chemical Society* **2000,** *122* (50), 12497-12506.
33. Santos, P. C. D., B. subtilis as a Model for Studying the Assembly of Fe–S Clusters in Gram-Positive Bacteria. In *Methods in Enzymolology*, 2017; Vol. 595, p 186.
34. Francesca D'Angelo, E. F.-F., Pierre Simon Garcia, Helena Shomar, Martin Pelosse, Rita Rebelo Manuel, Ferhat Büke, Siyi Liu, Niels van den Broek, Nicolas Duraffourg, Carol de Ram, Martin Pabst, Emmanuelle Bouveret, Simonetta Gribaldo, Béatrice Py, Sandrine Ollagnier de Choudens, Frédéric Barras, Gregory Bokinsky, Cellular assays identify barriers impeding iron-sulfur enzyme activity in a non-native prokaryotic host. *eLIFE* **2022,** (11).
35. Fleischhacker, A. S.; Stubna, A.; Hsueh, K. L.; Guo, Y.; Teter, S. J.; Rose, J. C.; Brunold, T. C.; Markley, J. L.; Munck, E.; Kiley, P. J., Characterization of the [2Fe-2S] cluster of Escherichia coli transcription factor IscR. *Biochemistry* **2012,** *51* (22), 4453-62.
36. Ferecatu, I.; Goncalves, S.; Golinelli-Cohen, M. P.; Clemancey, M.; Martelli, A.; Riquier, S.; Guittet, E.; Latour, J. M.; Puccio, H.; Drapier, J. C.; Lescop, E.; Bouton, C., The diabetes drug target MitoNEET governs a novel trafficking pathway to rebuild an Fe-S cluster into cytosolic aconitase/iron regulatory protein 1. *J Biol Chem* **2014,** *289* (41), 28070-86.
37. Wolfe, M. D.; Altier, D. J.; Stubna, A.; Popescu, C. V.; Munck, E.; Lipscomb, J. D., Benzoate 1,2-dioxygenase from Pseudomonas putida: single turnover kinetics and regulation of a two-component Rieske dioxygenase. *Biochemistry* **2002,** *41* (30), 9611-26.
38. Stegmaier, K.; Blinn, C. M.; Bechtel, D. F.; Greth, C.; Auerbach, H.; Muller, C. S.; Jakob, V.; Reijerse, E. J.; Netz, D. J. A.; Schunemann, V.; Pierik, A. J., Apd1 and Aim32 Are Prototypes of Bishistidinyl-Coordinated Non-Rieske [2Fe-2S] Proteins. *J Am Chem Soc* **2019,** *141* (14), 5753-5765.
39. Volbeda, A.; Martinez, M. T. P.; Crack, J. C.; Amara, P.; Gigarel, O.; Munnoch, J. T.; Hutchings, M. I.; Darnault, C.; Le Brun, N. E.; Fontecilla-Camps, J. C., Crystal Structure of the Transcription Regulator RsrR Reveals a [2Fe-2S] Cluster Coordinated by Cys, Glu, and His Residues. *J Am Chem Soc* **2019,** *141* (6), 2367-2375.
40. Munnoch, J. T.; Martinez, M. T.; Svistunenko, D. A.; Crack, J. C.; Le Brun, N. E.; Hutchings, M. I., Characterization of a putative NsrR homologue in Streptomyces venezuelae reveals a new member of the Rrf2 superfamily. *Sci Rep* **2016,** *6*, 31597.
41. Vinella, D.; Brochier-Armanet, C.; Loiseau, L.; Talla, E.; Barras, F., Iron-sulfur (Fe/S) protein biogenesis: phylogenomic and genetic studies of A-type carriers. *PLoS Genet* **2009,** *5* (5), e1000497.
42. Tan, G.; Lu, J.; Bitoun, J. P.; Huang, H.; Ding, H., IscA/SufA paralogues are required for the [4Fe-4S] cluster assembly in enzymes of multiple physiological pathways in Escherichia coli under aerobic growth conditions. *Biochem J* **2009,** *420* (3), 463-72.
43. Wang, W.; Huang, H.; Tan, G.; Si, F.; Liu, M.; Landry, A. P.; Lu, J.; Ding, H., In vivo evidence for the iron-binding activity of an iron-sulfur cluster assembly protein IscA in Escherichia coli. *Biochem J* **2010,** *432* (3), 429-36.
44. Hasnat, M. A.; Zupok, A.; Olas, J. J.; Mueller-Roeber, B.; Leimkuhler, S., A-Type Carrier Proteins Are Involved in [4Fe-4S] Cluster Insertion into the Radical S-Adenosylmethionine

Protein MoaA for the Synthesis of Active Molybdoenzymes. *J Bacteriol* **2021,** *203* (12), e0008621.
45. Beilschmidt, L. K.; Ollagnier de Choudens, S.; Fournier, M.; Sanakis, I.; Hograindleur, M. A.; Clemancey, M.; Blondin, G.; Schmucker, S.; Eisenmann, A.; Weiss, A.; Koebel, P.; Messaddeq, N.; Puccio, H.; Martelli, A., ISCA1 is essential for mitochondrial Fe4S4 biogenesis in vivo. *Nat Commun* **2017,** *8*, 15124.
46. Muhlenhoff, U.; Richter, N.; Pines, O.; Pierik, A. J.; Lill, R., Specialized function of yeast Isa1 and Isa2 proteins in the maturation of mitochondrial [4Fe-4S] proteins. *J Biol Chem* **2011,** *286* (48), 41205-16.
47. Weiler, B. D.; Bruck, M. C.; Kothe, I.; Bill, E.; Lill, R.; Muhlenhoff, U., Mitochondrial [4Fe-4S] protein assembly involves reductive [2Fe-2S] cluster fusion on ISCA1-ISCA2 by electron flow from ferredoxin FDX2. *Proc Natl Acad Sci U S A* **2020,** *117* (34), 20555-20565.
48. Vinella, D.; Loiseau, L.; Ollagnier de Choudens, S.; Fontecave, M.; Barras, F., In vivo [Fe-S] cluster acquisition by IscR and NsrR, two stress regulators in Escherichia coli. *Mol Microbiol* **2013,** *87* (3), 493-508.
49. Gerstel, A.; Zamarreno Beas, J.; Duverger, Y.; Bouveret, E.; Barras, F.; Py, B., Oxidative stress antagonizes fluoroquinolone drug sensitivity via the SoxR-SUF Fe-S cluster homeostatic axis. *PLoS Genet* **2020,** *16* (11), e1009198.
50. Veronesi, G.; Pérard, J.; Clémancey, M.; Gerez, C.; Duverger, Y.; Kieffer, I.; Barras, F.; Gambarelli, S.; Blondin, G.; de Choudens, S. O., A multidisciplinary analysis of the as-isolated Escherichia coli SufBC₂D complex reveals the presence of two new iron-sulfur clusters. *bioRxiv* **2022**, 2022.03.29.486248.

TOC

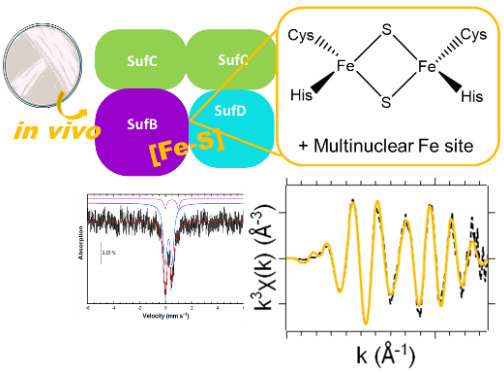

Synopsis: Utilization of diverse spectroscopies to characterize the native Fe-S cluster of the $SufBC_2D$ complex.